Int. J. Electrochem. Sci., 12 **(2017)** 7702 – 7711, doi: 10.20964/2017.08.03

International Journal of
ELECTROCHEMICAL
SCIENCE
www.electrochemsci.org

Electrodeposition of a Zn-MoS_2 Composite Film for the Catalytic Transesterification of Soybean Oil to Biodiesel

Zhenxu Huang[1,*], *Haijie Sun*[1], *Hairong Gao*[1], *Xianru Pei*[1] *and Shiqian Wei*[2,*]

[1] College of Chemistry and Chemical Engineering, Zhengzhou Normal University, No.6 Yingcai Rd, Zhengzhou, Henan, 450040 P.R. China
[2] Journal Editorial Office, Xuchang University, No.88 Bayi Rd, Xuchang, Henan, 461002 P.R. China
[*]E-mail: zhenxuhuang@foxmail.com

Received: 10 April 2017 / *Accepted:* 22 May 2017 / *Published:* 12 July 2017

This study explored an efficient catalyst for the production of biodiesel. Zinc sulfate was electrodeposited in a chloride bath containing uniformly dispersed MoS_2 nanoparticles to obtain a Zn-MoS_2 composite catalyst. Cyclic voltammetry (CV) and linear polarization were employed to investigate the Zn-MoS_2 catalyst deposition process. The effects of the catalyst stability, catalyst loading, reaction time and molar ratio of methanol to oil were studied. The optimized catalytic activity was obtained at 10% Zn-MoS_2 catalyst loading. The Zn-MoS_2 catalyst could be easily recovered and reused without exhibiting apparent activity loss.

Keywords: Catalyst; MoS_2; Znic; Soybean; Biodiesel; Electrodeposition

1. INTRODUCTION

Since biodiesel based on fatty acid alkyl esters (FAAEs) is not only renewable but also produces comparatively lower greenhouse gas and particulate matter emissions, it is regarded as a competitive substitute for traditional diesel fuel [1-4]. In addition, it is highly biodegradable and lubricating and possesses a high flash point and cetane number [5, 6]. With respect to the routine production of biodiesel, triglycerides in animal fat or vegetable oil undergo transesterification over a proper catalyst with the addition of ethanol or methanol to yield FAAEs and the main by-product, glycerol [7]. Typically, the catalysis of triglyceride transesterification to yield FAAEs and the by-product is realized by utilizing enzymes, strong acid or strong base [8]. Additionally, the chemical equilibrium can be shifted to the product mixture with excess alcohol [9, 10].

Triglycerides in agro-based oils are undergo transesterification, mainly over homogeneous alkali catalysts that can enhance the reaction rate even under modest reaction conditions, to yield industrial biodiesel. Since glycerol and the catalyst must be washed in the process, there are substantial amounts of wastewater produced during the reaction [11]. Furthermore, a stable emulsion and soap are produced, resulting in continuous water contamination and yield losses. Heterogeneous solid acid and/or solid base catalysts are green, recyclable, easily separated, and can yield clean biodiesel and glycerol while maintaining a heterogeneous nature. Therefore, there is no need for the products to be washed or purified in the processing stages. Nevertheless, longer reaction times, higher pressures and temperatures, and larger molar amounts of esterifying agents are needed for the aforementioned catalysts to address the problem of diffusion that is caused by the formation of three phases of the reactants [12-14]. Increased specific surface areas and pore sizes for the active species can be provided by catalyst supports or structural promoters, where anchoring and reactions with large triglyceride molecules can occur, thus solving the problem of mass transfer [15]. In addition, the catalyst would have a longer life span and be more mechanically stable with the use of catalyst supports or structural promoters. Current enzyme catalytic processes are unappealing for the commercial production of biodiesel, since they not only show lower conversion rates but also have expensive production processes.

To protect ferrous materials from corrosion, zinc coatings have gained widespread application, since they can serve as a self-sacrificial anodic protective layer and physically protect against the aggressive surroundings. The electrodepositions of zinc coatings from various electrolytes have been a recent focus, where diverse organic and inorganic compounds have been added to achieve enhanced deposition features, corrosion performances and morphologies [16-18]. To make the terminal composite material stronger and more wear resistant, MoS_2 particles are typically dispersed into nickel, copper or other metal matrices [19-21].

This work employed an electrodeposition technique to obtain a solid Zn-MoS catalyst for the transesterification of soybean oil with methanol. In addition, it is distinct in the use of heterogeneous Zn-MoS during the transesterification reaction. Herein, the conversion to methyl esters was considered to evaluate the catalytic activity of this catalyst during the transesterification of soybean oil.

2. EXPERIMENTAL SECTIONS

2.1. Reagents

Refined soybean oil used as raw material for the transesterification reaction was obtained from a local market (Zhengzhou, China). Based on measurements by GC (Shimadzu DC-9A), the distribution of the fatty acids was determined to be: linolenic, linoleic, oleic, stearic and palmitic acid at percentages of 5.9%, 49.3%, 26.5%, 5.8% and 12.1%, respectively, as well as other fatty acids in trace levels. Based on the calculation of the saponification value (SV) of 192.6 mg KOH/g, the acid value of the soybean oil was measured to be below 0.1 mg KOH/g, with an average molecular weight of 874 g/mol. All other reagents were purchased and of analytical grade.

2.2. Electrodeposition of the Zn-MoS_2 composite catalyst

The cathode substrate employed was a mild steel foil with dimensions of 1 × 1 × 0.1 cm. After mechanical polishing and trichloroethylene degreasing, the mild steel was washed with water and subjected to a plating procedure. The anode used was a 99.9% Zn plate, which was then dipped into HCl (10%) for several seconds to activate its surface each time prior to washing with water and utilization in the tests. The cathode and anode with the same sizes were employed during the electrodeposition procedure conducted under a constant current density (4 A/dm^2) for a deposition of 20 min. The coatings were deposited via DC currents on a model PS-618 potentiostat/galvanostat. The electrolyte was stirred at 300 rpm during the deposition procedure. Table 1 lists the composition of the plating bath.

Table 1. Plating bath composition

$ZnSO_4 \cdot 7H_2O$	200 (in g/L)	NaCl	20 (in g/L)
Na_2SO_4	30 (in g/L)	H_3BO_3	15 (in g/L)
SDS (surfactant)	0.5 (in g/L)	MoS_2	0-1 (in g/L)

2.3. Catalyst characterization

A zeta potential analyzer (Zeta Plus™) was employed to detect the zeta potential (surface charge) of the MoS_2 particles in the plating bath at 25 °C. The average mobility of the particles was reflected by the zeta potential obtained. Cu-Kα radiation ($\lambda = 0.1540$ nm) was applied in an X-ray diffractometer (Philips TW 3710) to analyze the electrodeposits via X-ray diffraction (XRD) measurements. The parameters for the working Ni filter were 40 kV and 30 mA. The X-ray data were obtained to assess the preferred orientations of the electrodeposits. A reference MoS_2 ICDD-JCPDS card number 39-1492 and reference zinc ICDD-JCPDS card number 87-0713 were employed for calculations. Potentiodynamic polarization and cyclic voltammetry were performed using a CHI660C electrochemical work station. The measurements were performed using a conventional three-electrode cell, in which the test sample was placed in a Teflon sample holder with an exposed surface area to the corrosive medium of approximately 1 cm^2. A platinum wire served as counter electrode, and an SCE electrode was used as the reference electrode. Cyclic voltammetry was conducted in a 3.5 M NaCl solution at a scan rate of 50 mV/s.

2.4. Transesterification procedures

The transesterification of soybean oil with methanol was investigated to study the activity of the catalysts. Supplied with a magnetic stirrer and a reflux condenser, a round-bottom flask (250 mL) was employed to perform all the transesterification experiments. Typically, the reagents in the reactor included the freshly prepared catalyst, anhydrous methanol (35 mL) and soybean oil (16 g). Under methanol refluxing conditions, the catalyzed transesterification was conducted for a fixed time. To

prevent mass transfer limitations, the mixed solution was stirred at a varied rate and refluxed during the entire reaction process. The catalyst loading, reaction time, methanol/oil ratio (10:1, 20:1, 30:1, 40:1. 50:1 and 60:1) and other parameters were changed during the experiments. The mixed solution was filtered and separated to yield the solid catalyst after the reaction finished. On the other hand, a rotary evaporator was employed to recover the remaining methanol at 343 K under vacuum before following analyses. A series of successive and reversible reactions occurred during the transesterification, and the conversion is described as follows: triglyceride to diglyceride to monoglyceride to glycerin to fatty acid methyl ester. With the production of a methyl ester, the liberation of a free hydroxyl group occurs. Thus, it can be concluded that the hydroxyl content of the liquid phase at this stage would increase as the amount of methyl ester increased if the absolute removal of excessive methanol was achieved. The free hydroxyl contents on the free and bound glycerin in the reaction mixture were measured to obtain the molar oil conversion, and this data was calculated by averaging no less than two tests with errors below 3%. Chromatographic analysis was employed to cross-check and calibrate this technique. Models for the free fatty acid, oleic acid, and water were deliberately introduced to the soybean oil to analyze the effects of water and the free fatty acid in the feedstock. After the reaction, the mixture was collected and centrifuged to separate the solid catalyst. The upper layer was collected for further purification. After evaporation of methanol, the methyl ester content in the upper layer was quantified using a GC-2010 gas chromatograph connected to a CP-FFAP capillary column. The column temperature was kept at 180 °C for 0.5 min, raised to 250 °C at 10 °C/min and maintained at this temperature for 6 min. The temperatures of the injector and detector were set to 250 °C and 260 °C, respectively. The biodiesel yield was calculated from the equation below:

$$Biodiesel\ Yield(\%) = \frac{Total\ amount\ of\ \ five\ methyl\ ester(M)}{Ch\arg e\ amount\ of\ \ triglycerides(M)\times 3\times 100\%}$$

3. RESULTS AND DISCUSSION

The ZetaPlus system possesses a laser beam that passes through the specimen in a cell with an electric field supplied by its two electrodes. Thus, the zeta potential analyzer measures both the direction and the velocity of the particles under the influence of a known electric field and then calculates the mobility and zeta potential from this information. The relationship between the mobility and zeta potential (ζ) relies on the applied theoretical model. The direction that these values move is a clear indication of the sign of the charge they carry. Their velocity is proportional to the magnitude of the charge. The nature and magnitude of the charge are a function of the pH value [22, 23]. This work utilized calculations using the Smoluchowski limit. In theory, solid particles that enter an aqueous interface show a tendency to polarize and exhibit an electrical charge. Fig. 1 displays the zeta potentials obtained in solutions at various pH values to explore the adsorption of the charged groups onto the particles. As the pH value dropped, there was an increase in the zeta potential, possibly due to H^+ ions adsorbing onto the particle surfaces.

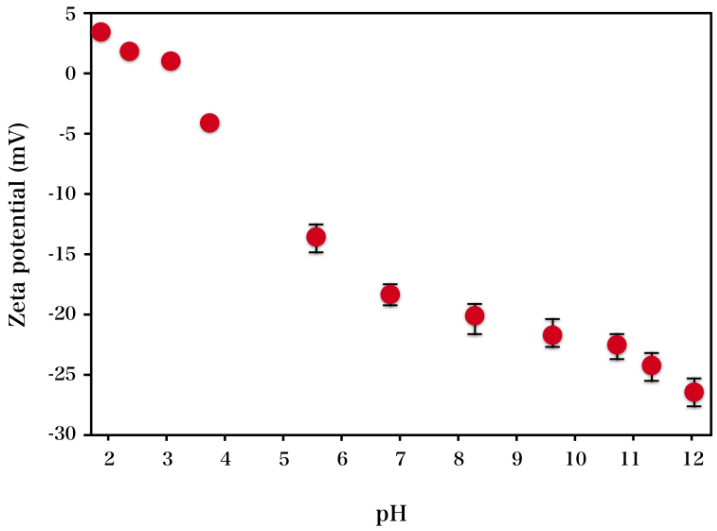

Figure 1. Zeta potential measurements of the MoS_2 particles in aqueous solution assayed at various pH values.

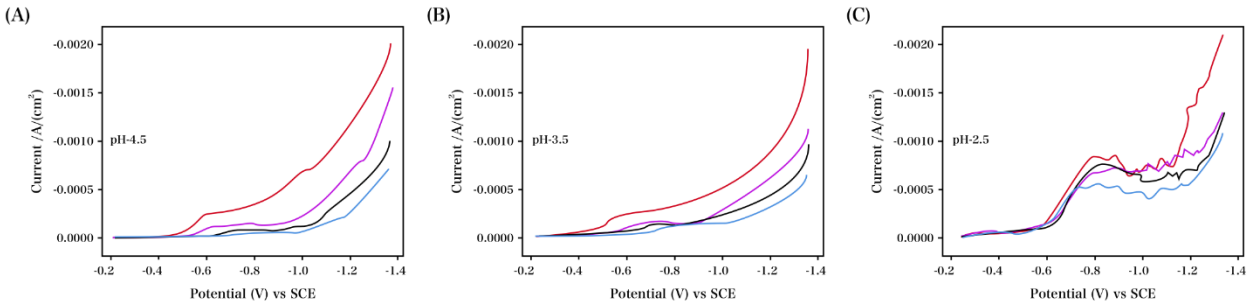

Figure 2. Catholic polarization profiles on the steel electrode in the blank solution (plating bath in the absence of zinc) containing various quantities of MoS_2 at various pH values: (A) 4.5, (B) 3.5 and (C) 2.5.

We performed cathodic polarization tests to explore the influence of the MoS_2 particles on the reduction in the deposition procedure, with the cathodic polarization characterized with respect to the blank and zinc solutions in the presence and absence of MoS_2 at a scan rate of 0.01 V/s. The cathodic sweeps recorded for the blank solution at various MoS_2 concentrations and pH values are shown in Fig. 2A-C. In Fig. 2A, it can be seen that the first limiting current density plateau is related to the hydrogen evolution reaction (HER) followed from water reduction.

$$H_3O^+ + 2e^- \rightarrow H_2 + OH^-$$

$$2H_2O + 2e^- \rightarrow H_2 + 2OH^-$$

As the MoS_2 particles at various pH values were added into the blank solution, there were not any further changes. However, a surface obstruction appeared on the electrode, leading to the hydrogen evolution reaction (HER). It was found that the MoS_2 particles adsorbed onto the cathode, suggesting the successful transfer of MoS_2, which was dispersed in the bulk solution, onto the surface of the

electrode. With a decrease of the pH value, there was an increase in the adsorption of H^+ ions and then an increase in the zeta potential. Many factors can influence the transportation of the MoS_2 particles on the cathode, such as electrophoresis, mechanical entrapment, adsorption, and convection diffusion. Many models have been reported in the literature to explain these mechanisms [24-26].

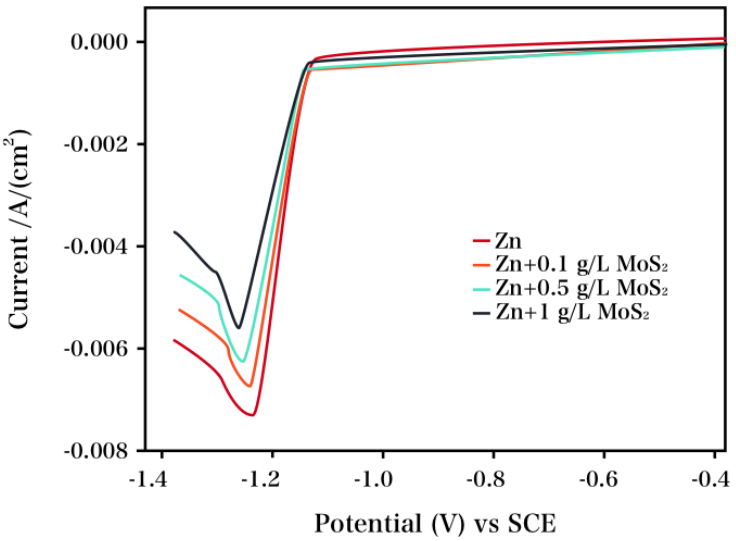

Figure 3. Cathodic polarization profiles for the deposition of Zn-MoS_2 and zinc from the plating bath.

The cathodic polarization performance of the Zn-MoS_2 electrolyte at pH 3.5 with various concentrations of MoS_2 was studied, as characterized in Fig. 3. In comparison with the deposition of the zinc, the reduction potential of Zn^{2+} was observed at a more negative potential as the amount of MoS_2 increased. Moreover, the reaction solution containing MoS_2 (1 g/L) made this potential feature become sharper. Thus, it was found that the cathodic polarization was enhanced by the addition of MoS_2 into the electrolyte, while the slope was unchanged. Here, the deposition of Zn^{2+} ions was obstructed by MoS_2 absorbed onto the surface of the cathode, while the electrochemical reaction mechanism remained primarily unaffected. The physical dispersion and electrophoretic migration of the particles in the electrolyte facilitated incorporation of particles into the Zn metallic matrix [27]. The polarization values obtained using higher concentrations of MoS_2 were almost identical to those of the bath solution containing 1 g/L MoS_2, possibly due to the aggregation of MoS_2 at the bottom of the cell during electrodeposition process, which led to a decrease in the effective concentration of the MoS_2 particles.

The effect of the concentration of MoS_2 particles on the zinc electrodeposition in the bath solution (pH 3.5) was characterized via CV, as displayed in Fig. 4. For the CV measurements, the scan rate was 0.01 V/s, and the scanning began at −0.4 V in the negative direction and then was reversed at −1.4 V back to −0.4 V. The substantial reduction of Zn^{2+} to Zn was correlated with the reduction peak I_c. Upon reversing the potential sweep, the deposit-induced oxidation peak I_a appeared. In the original zinc solution, the reduction of zinc was activated at −1.14 V (versus SCE). In comparison,

with the electrolyte containing 0.1, 0.5, and 1 g/L MoS_2, the reduction of zinc was activated at −1.145, −1.152, and −1.165 V, respectively. At 0.1 g/L MoS_2, there was a decrease of I_a observed for the electrooxidation of the deposit, while nearly no variation was observed for the electroreduction peak. The decreasing of the current response may attribute to the decreasing of the deposited area when the presence of the MoS_2 particles [28]. As the concentration of MoS_2 was increased, there was a slight shift in the reduction to a more negative potential and a decrease in the peak reduction current (I_c). Meanwhile, with an increase in the MoS_2 concentration, there was a decrease in the electrooxidation peak current (I_a), possibly attributed to MoS_2-induced surface obstruction of the electrode. There was a decrease in the anodic dissolution rate, possibly due to the MoS_2 particles in the deposit providing a chemically stable composite. As the direction of the potential sweep was reversed, the critical potential value for nucleation was determined to be −1.08 V (versus. SCE), which was the same for either pure zinc or the composite electrolytes, suggesting that there were no further reactions during the nucleation of zinc.

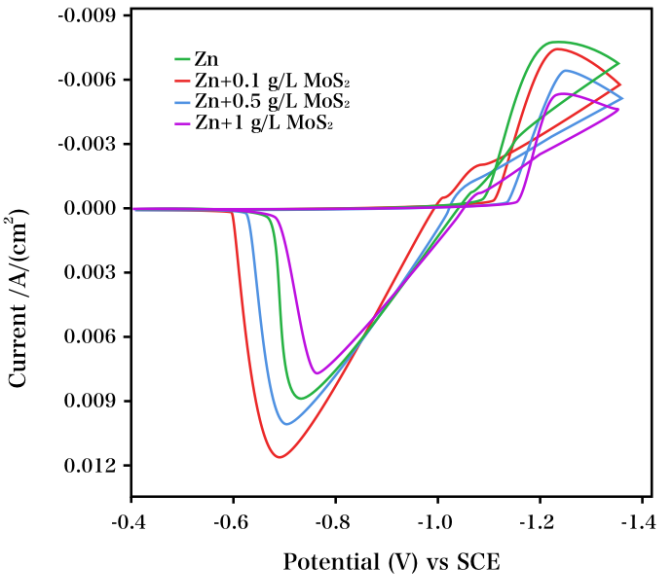

Figure 4. CV profiles for the zinc and Zn-MoS_2 plating baths.

A vital factor during the transesterification process is the molar ratio of methanol to oil. Due to the reversibility of triglyceride transesterification, the equilibrium could be forced towards the products by excess methanol, resulting in an enhanced production of methyl esters [29, 30]. The effect of the molar ratio of methanol to oil on the conversion over the Zn-MoS_2 catalyst is displayed in Table 2, where the conversion with Zn-MoS_2 was enhanced as the molar ratio of methanol to oil increased from 10:1 to 50:1, with a plateau observed at a ratio of 60:1. Therefore, the optimal methanol/oil molar ratio was 50:1, where a conversion of 84.5% was obtained. Through a facile distillation under vacuum, the excessive quantity of employed methanol was recovered and employed again during the following transesterification reaction.

The effect of the catalyst loading on the soybean oil conversion was studied, as illustrated in Table 2. The reaction time and methanol/oil molar ratio were 60 h and 50:1, respectively. There was no product yield for the transesterification in the absence of Zn-MoS_2. As the amount (2 wt.%) of the Zn-MoS_2 catalyst was increased up to 8 wt.%, there was an apparent increase in the soybean oil conversion as presumed. Further increased the catalyst leaded a decreasing of the transesterification result. It can be attributed to the hidden the catalytic sites [31, 32]. Here, a maximal conversion of 84.5% was obtained, and thus, 8 wt.% was fixed as the optimal amount of catalyst. The increase in the availability of the catalytically active sites requires a higher catalyst loading. The triglycerides could not be completely converted into methyl esters with an inadequate quantity of Zn-MoS_2. At higher amounts than the optimized quantity, there was only a slight increase in the conversion. In addition, the viscosity of the mixed solution would increase when a substantial amount of the Zn-MoS_2 catalyst was present, and eventually, the mass transfer resistance would become a detriment during the heterogeneous reaction. Hence, ca. 8 wt.% was set as the optimized amount of catalyst in the transesterification process.

Table 2. Optimization **of** the reaction conditions for the transesterification of soybean oil over the Zn-MoS_2 catalyst.

No.	Methanol/oil (molar ratio)	Catalyst loading (wt.%)	Reaction time (h)	Conversion (%)
1	10:1	10	60	24.3
2	20:1	10	60	44.5
3	30:1	10	60	65.1
4	40:1	10	60	72.0
5	50:1	10	60	83.6
6	60:1	10	60	84.1
7	50:1	2	60	58.9
8	50:1	4	60	60.0
9	50:1	6	60	81.5
10	50:1	8	60	84.5
11	50:1	10	60	78.2
12	50:1	8	20	31.6
13	50:1	8	30	45.4
14	50:1	8	40	62.8
15	50:1	8	50	81.6
16	50:1	8	60	82.0

The conversions to methyl esters with various reaction times (1 to 60 h) are displayed in Table 2. The formation of methyl ester was barely observed over the first hour of the reaction. At 10 and 40 h, there was an enhancement in the conversion up to 31.6% and 62.8%, respectively. Furthermore, an increase to 81.6% was observed when the reaction time was lengthened to 50 h, with almost no further change over 50 h. Therefore, the most transesterification reaction can be finished within 50 h.

A vital factor for a heterogeneous catalyst in industry is its stability. The solid catalyst was filtrated prior to thorough washing with methanol and petroleum ether to remove the polar and non-polar surface-adsorbed compounds and was then calcinated for 5 h at 823 K to investigate its recyclability. Then, the recovered catalyst was employed for a new transesterification reaction. The reusability of the catalyst was examined under the optimal conditions. The conversions obtained after 1, 2, 3, 4, and 5 cycles of application were 84.1%, 82.3%, 75.6%, 71.6%, and 68.3%, respectively. Hence, this catalyst was reusable with insignificant activity loss.

4. CONCLUSIONS

This work employed an electrodeposition approach to obtain a Zn-MoS_2 composite catalyst, which significantly promoted the catalytic activity of a transesterification process. The optimized loading for this catalyst was 10%, corresponding to an oil conversion under methanol refluxing conditions of 84.1% at a molar ratio of methanol to oil of 50:1. The Zn-MoS_2 catalyst was found to be highly stable and exhibit no prominent catalytic activity loss even after 5 cycles.

References

1. F. Ma and M. Hanna, *Bioresource Technology*, 70 (1999) 1.
2. S. Ghadge and H. Raheman, *Biomass and Bioenergy*, 28 (2005) 601.
3. H. Fukuda, A. Kondo and H. Noda, *Journal of Bioscience and Bioengineering*, 92 (2001) 405.
4. M. Dorado, E. Ballesteros, J. Arnal, J. Gomez and F. Lopez, *Fuel*, 82 (2003) 1311.
5. T. Ryan Iii, L. Dodge and T. Callahan, *Journal of the American Oil Chemists Society*, 61 (1984) 1610.
6. R. Alcantara, J. Amores, L. Canoira, E. Fidalgo, M. Franco and A. Navarro, *Biomass and Bioenergy*, 18 (2000) 515.
7. M. Graboski and R. McCormick, *Progress in Energy and Combustion Science*, 24 (1998) 125.
8. J. Encinar, J. Gonzalez and A. Rodríguez-Reinares, *Ind. Eng. Chem. Res.*, 44 (2005) 5491.
9. J. Van Gerpen, *Fuel Processing Technology*, 86 (2005) 1097.
10. M. Haas, *Fuel Processing Technology*, 86 (2005) 1087.
11. H. Kim, B. Kang, M. Kim, Y. Park, D. Kim, J. Lee and K. Lee, *Catalysis Today*, 93 (2004) 315.
12. T. Dossin, M. Reyniers, R. Berger and G. Marin, *Appl. Ctatl. B-Environ.*, 67 (2006) 136.
13. Y. Ono and T. Baba, *Catalysis Today*, 38 (1997) 321.
14. J. Clark and D. Macquarrie, *Chemical Society Reviews*, 25 (1996) 303.
15. M. Zabeti, W. Daud and M. Aroua, *Fuel Processing Technology*, 90 (2009) 770.
16. X. Xia, I. Zhitomirsky and J. McDermid, *Journal of Materials Processing Technology*, 209 (2009) 2632.
17. M. Ilieva, S. Ivanov and V. Tsakova, *Journal of Applied Electrochemistry*, 38 (2008) 63.
18. H. Zheng, A. Maozhong and L.U. Junfeng, *Rare Metals*, 25 (2006) 174.
19. V. Fox, N. Renevier, D. Teer, J. Hampshire and V. Rigato, *Surface and Coatings Technology*, 116 (1999) 492.
20. N. Renevier, H. Oosterling, U. König, H. Dautzenberg, B. Kim, L. Geppert, F. Koopmans and J. Leopold, *Surface and Coatings Technology*, 172 (2003) 13.
21. J. Lince, H. Kim, P. Adams, D. Dickrell and M. Dugger, *Thin Solid Films*, 517 (2009) 5516.

22. S. Salgin, U. Salgin and N. Soyer, *Int. J. Electrochem. Sc.*, 8 (2013) 4073.
23. S. Singh, V. Srivastava and I. Mall, *RSC Advances*, 3 (2013) 16426.
24. N. Guglielmi, *Journal of the Electrochemical Society*, 119 (1972) 1009.
25. J. Celis, J. Roos and C. Buelens, *Journal of the Electrochemical Society*, 134 (1987) 1402.
26. J. Fransaer, J. Celis and J. Roos, *Journal of the Electrochemical Society*, 139 (1992) 413.
27. Z. Liu, S. El Abedin and F. Endres, *Phys Chem Chem Phys*, 17 (2015) 15945.
28. B. Łosiewicz, G. Dercz and M. Popczyk, *Solid State Phenomena*, 228 (2015) 125.
29. M. Veillette, A. Giroir-Fendler, N. Faucheux and M. Heitz, *Chem. Eng. J.*, 308 (2017) 101.
30. R. Murray and H. Furlonge, *International Journal of Global Energy Issues*, 39 (2016) 340.
31. A. Demirbas, *Energy Sources Part A Recovery Utilization & Environmental Effects*, 38 (2016) 1890.
32. M. García-Jarana, J. Sánchez-Oneto, J. Portela, L. Casas, C. Mantell and E. Ossa, *Korean J. Chem. Eng.*, (2016) 1.